

# Project 3 - FYS4150

Nanna Bryne, Johan Mylius Kroken, Vetle A. Vikenes  
(Dated: October 26, 2022)

We provide an overview of how to structure a scientific report. For concreteness, we consider the example of writing a report about an implementation of the midpoint rule of integration. For each section of the report we briefly discuss what the purpose of the given section is. We also provide examples of how to properly include equations, tables, algorithms, figures and references.

## I. INTRODUCTION

### Things left to do:

- Write abstract
- Write conclusion
- Finish discussion
- Rewrite results, or change it up so we don't repeat ourselves.
- Check figure captions (conventional writing, references etc)
- Read through most of the text for typos and coherence

Trapping charged particles is a common and useful method in order to perform various measurements and experiments. A natural starting point would be to create a three-dimensional electric potential which pulls the particles towards a center. According to Earnshaw's theorem [3], keeping a charged particle in stable equilibrium with an electrostatic force alone is not possible. One way around this is to use a strong homogeneous axial magnetic field together with a quadrupole electric field. The former incarcerates the particle(s) radially, whereas the latter confines the particles radially. A device of such a structure is called a "Penning trap" and was first built by Hans Georg Dehmelt under the influence of Frans Michel Penning's work [2]. The Lorentz force  $\mathbf{F}$  acting on a particle with charge  $q$  that is subjected to this electric field and a magnetic field,  $\mathbf{B}$ , is given by

$$\mathbf{F} = q\mathbf{E} + q\mathbf{v} \times \mathbf{B}, \quad (1)$$

where  $\mathbf{v}$  is the particle's velocity. Suppose the particle has mass  $m$ , then Newton's second law gives us the equation of motion for the particle:

$$\frac{d\mathbf{v}}{dt} = \frac{\mathbf{F}}{m} \Rightarrow \frac{d^2\mathbf{r}}{dt^2} = \frac{q}{m}(\mathbf{E} + \mathbf{v} \times \mathbf{B}). \quad (2)$$

The external electric field is related to the potential through  $\mathbf{E} = -\nabla V$ . By choosing a particular electric potential and magnetic field, we can solve equation (2) to predict the motion of a single particle inside a Penning trap. In reality one is often concerned with storing multiple particles, not just a single one. This introduces

Coulomb interactions between the particles, and the resulting equations of motion will then be much more cumbersome to tackle analytically. To study the motion of the trapped particles we will therefore resort to numerical integration methods.

**Mention that we use Calcium ions only in the introduction?**

Equation (2) can be split into two ordinary differential equations (ODEs) that we can solve numerically. The two methods we will consider are forward Euler (FE) and fourth order Runge-Kutta (RK4) **citation?**. FE requires fewer floating point operations (FLOPs) per iteration compared to RK4, but RK4 provides a much more accurate result at a given step size **replace "more accurate" with "smaller error" in previous sentence?**. By solving the equations of motion for a single particle in the Penning trap analytically we can estimate the error of the two numerical schemes. Estimating the accuracy of our solver when particle interactions are present is a difficult task in the absence of analytical expressions. The single particle case will therefore provide us with key insight to the validity of our solvers. By simulating two particles in the trap both with and without interactions, we can use the single particle results to evaluate our implementation.

**New resonance explanation:**

When the basics of our solver have been studied we want to explore physical properties of the Penning trap. We will limit our analysis to a study of resonance phenomena in the trap. To do this we will subject the particles to a time dependent electric potential, which oscillates at a certain applied frequency. If resonance occurs we expect that particles eventually escape the trap, when their distances from the origin exceeds the extent of the trap itself. By devising a scheme to quantify the escape of particles we can find the frequencies at which resonance occurs, and possibly relate this to the physical properties (**/parameters/quantities?**) of the Penning trap. The final question we then want to answer is whether particle interactions affect the onset of resonance, and if so, how.

**Old resonance explanation:**

In addition, we will investigate the effect of adding an oscillating time-dependent perturbation to the external electric potential  $V$ . This is indeed similar to another approach for particle storage, named the Paul trap, in which the oscillating field is used instead of the magnetic field. The combined ion trap, the combination of these two structures, allows for storage of oppositely charged

particles, but is vulnerable to some ranges of oscillation frequencies and amplitudes (CHECK THIS).

In this report we begin by introducing the Penning trap in section II. Here we present the setup of the trap and the resulting equations of motion for particles in the trap. We derive the analytical solutions for a single particle in section II B and describe the modifications to the equations of motion when interactions between multiple particles is included in section II C.

In section III A we present our numerical solver. We present our choice of parameters for the trap and the initial conditions for testing in Sections III B and III C respectively. In section III D we present the analysis for a single particle, as well as two particles in the trap. Section III E focuses on our investigation of resonance phenomena in the trap.

The results of our investigations are presented in section IV. Finally, we discuss our results and present our conclusions in sections V and VI respectively.

## II. THE PENNING TRAP

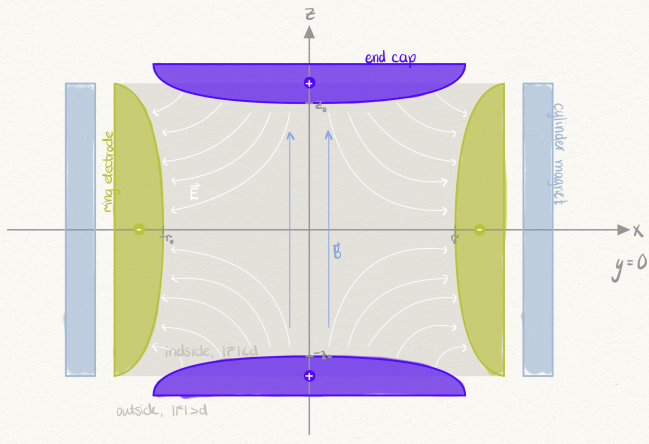


FIG. 1. Schematic of the Penning trap. The cross-section is in the  $xz$ -plane. The ring electrode (green) and end caps (dark blue) sets the inhomogeneous electric field (white arrows). The homogeneous magnetic field (blue arrows) is resulting from the cylinder magnet (light blue) outside of the trap. For simplicity, we will assume that the trap extends the distance  $d$  in all directions, see text for further details.

We consider an ideal Penning trap in three dimensions, with a schematic of the trap shown in figure 1.

### A. External electromagnetic fields

The electrodes in the Penning trap create an external electric field  $\mathbf{E}_{\text{ext}}$  defined by the potential

$$V(\mathbf{r}) = V(x, y, z) = \frac{V_0}{2d^2}(2z^2 - x^2 - y^2), \quad (3)$$

where  $V_0$  is the potential applied to the electrodes and  $d = \sqrt{z_0^2 + \frac{1}{2}r_0^2}$  is the characteristic dimension, where  $z_0$  is the distance between the centre and the endcap and  $r_0$  is the radius of the ring. The external electric field resulting from this potential is

$$\mathbf{E}_{\text{ext}} = -\nabla V = \frac{V_0}{d^2}(x, y, -2z), \quad (4)$$

which traps the particles in the  $z$ -direction. To contain the particles in the  $xy$ -plane, a constant homogeneous magnetic field  $\mathbf{B}_{\text{ext}}$  is imposed in the  $z$ -direction,

$$\mathbf{B}_{\text{ext}} = (0, 0, B_0). \quad (5)$$

As a simplification, we consider the trap as a sphere of radius  $d$ . We set the external fields to zero outside this region, so the electric field is

$$\mathbf{E}_{\text{ext}}(\mathbf{r}) = \begin{cases} \frac{V_0}{d^2}(x, y, -2z), & |\mathbf{r}| \leq d \\ (0, 0, 0), & |\mathbf{r}| > d \end{cases}, \quad (6)$$

and the magnetic field is

$$\mathbf{B}_{\text{ext}}(\mathbf{r}) = \begin{cases} (0, 0, B_0), & |\mathbf{r}| \leq d \\ (0, 0, 0), & |\mathbf{r}| > d \end{cases}. \quad (7)$$

For the analytical derivations that follow in this section (section II), we will assume that  $|\mathbf{r}| \leq d$  is fulfilled.

### B. Analytical solutions - Single particle

We begin by considering a single particle in the Penning trap. The Lorentz force is then governed by the external fields only, hence  $\mathbf{E} = \mathbf{E}_{\text{ext}}$  and  $\mathbf{B} = \mathbf{B}_{\text{ext}}$ . We use eq. (1) to compute the Lorentz force,

$$\begin{aligned} \mathbf{F} &= \frac{qV_0}{d^2}(x, y, -2z) + qB_0(\dot{y}, -\dot{x}, 0) \\ &= \frac{m}{2}\omega_z^2(x, y, -2z) + m\omega_0(\dot{y}, -\dot{x}, 0), \end{aligned} \quad (8)$$

where we defined  $\omega_0 \equiv \frac{qB_0}{m}$  and  $\omega_z^2 \equiv \frac{2qV_0}{md^2}$ . Using equation (2) gives us three equations of motion, one for each spatial component, which are

$$\ddot{x} - \omega_0 \dot{y} - \frac{1}{2}\omega_z^2 x = 0, \quad (9a)$$

$$\ddot{y} + \omega_0 \dot{x} - \frac{1}{2}\omega_z^2 y = 0, \quad (9b)$$

$$\ddot{z} + \omega_z^2 z = 0. \quad (9c)$$

The general solution of eq. (9c) is

$$z(t) = c_1 \cos(\omega_z t) + c_2 \sin(\omega_z t), \quad (10)$$

where  $c_1, c_2 \in \mathbb{R}$  are determined by initial conditions.

Equations (9a) and (9b) are coupled, so we introduce a complex function  $f(t) = x(t) + iy(t)$  to write them

as a single differential equation. Multiplying equation (9b) with  $i$  and adding it to equation (9a) we obtain the following:

$$\begin{aligned} \ddot{x} + i\ddot{y} + \omega_0(i\dot{x} - \dot{y}) - \frac{1}{2}\omega_z^2(x + iy) &= 0 \\ (\ddot{x} + i\ddot{y}) + i\omega_0(\dot{x} + i\dot{y}) - \frac{1}{2}\omega_z^2(x + iy) &= 0. \end{aligned} \quad (11)$$

We recognize the first and second parentheses as  $\ddot{f}$  and  $\dot{f}$ , respectively. The differential equation for  $f(t)$  is

$$\ddot{f} + i\omega_0\dot{f} - \frac{1}{2}\omega_z^2 f = 0, \quad (12)$$

which has the general solution

$$f(t) = A_+ e^{-i(\omega_+ t + \phi_+)} + A_- e^{-i(\omega_- t + \phi_-)}, \quad (13)$$

where  $\phi_+$  and  $\phi_-$  are constant phases,  $A_+$  and  $A_-$  are positive amplitudes and

$$\omega_{\pm} = \frac{\omega_0 \pm \sqrt{\omega_0^2 - 2\omega_z^2}}{2}. \quad (14)$$

The physical coordinates are then  $x(t) = \text{Re } f(t)$  and  $y(t) = \text{Im } f(t)$ . **The following sentence confuses me:** The  $\omega_+$  is the modified cyclotron frequency and the  $\omega_-$  is the magnetron frequency that composes the two modes in the orbital motion we will discuss later.

In order to have a bounded solution for the particle in the  $xy$ -plane, we must have  $|f(t)| < \infty$  as  $t \rightarrow \infty$ . We see from equation (13) that this condition is fulfilled if  $\omega_{\pm} \in \mathbb{R}$ . From equation (14), this translates to the following constraint on  $\omega_0$  and  $\omega_z$ :

$$\begin{aligned} \omega_0^2 &\geq 2\omega_z^2, \\ \frac{q}{m} &\geq \frac{4V_0}{(B_0 d)^2}, \end{aligned} \quad (15)$$

where we used the definitions of  $\omega_0$  and  $\omega_z$  to get a constraint relating the particle properties with the Penning trap parameters. This allows us to choose appropriate parameters for our Penning trap, depending on the mass of the particle we consider.

Knowing that the particles are bound in the  $xy$ -plane, we want to consider the upper and lower bounds,  $R_+$  and  $R_-$  respectively, on the particle's distance from the origin. With  $f(t)$  being a complex function, its magnitude is found by  $|f(t)| = \sqrt{f(t)f^*(t)}$ . Defining  $\alpha_{\pm} \equiv \omega_{\pm}t + \phi_{\pm}$  to simplify the expressions, we get

$$|f^2(t)| = A_+^2 + A_-^2 + A_+ A_- \left( e^{i(\alpha_+ - \alpha_-)} + e^{-i(\alpha_+ - \alpha_-)} \right) \quad (16)$$

Recognizing the sum of the exponentials as the cosine,  $|f(t)|$  becomes

$$|f(t)| = \sqrt{A_+^2 + A_-^2 + 2A_+ A_- \cos(\alpha_+ - \alpha_-)}. \quad (17)$$

The maximum distance from the origin,  $R_+$ , occurs when  $\alpha_+ - \alpha_- = 0 \implies \cos 0 = 1$ . Similarly, the minimum

distance,  $R_-$ , is achieved when  $\alpha_+ - \alpha_- = \pi \implies \cos \pi = -1$ . Equation (17) now gives us simple expression for the two bounds

$$R_+ = \sqrt{(A_+ + A_-)^2} = A_+ + A_-, \quad (18)$$

$$R_- = \sqrt{(A_+ - A_-)^2} = |A_+ - A_-|. \quad (19)$$

### C. Multiple particles

So far, we have only considered the presence of a single particle in the Penning trap. With multiple particles simultaneously present in the trap, each particle will now be affected by the Coulomb force from the other particles. The electric field at a point  $\mathbf{r}$  due to interactions,  $\mathbf{E}_{\text{int}}(\mathbf{r})$ , set up by  $N_p$  point charges  $\{q_1, q_2, \dots, q_{N_p}\}$  at positions  $\{\mathbf{r}_1, \mathbf{r}_2, \dots, \mathbf{r}_{N_p}\}$  is given by

$$\mathbf{E}_{\text{int}}(\mathbf{r}) = k_e \sum_{p=1}^{N_p} q_p \frac{\mathbf{r} - \mathbf{r}_p}{|\mathbf{r} - \mathbf{r}_p|^3}, \quad (20)$$

where  $k_e$  is Coulomb's constant.

The electric field contributing to the Lorentz force in equation (1) is then  $\mathbf{E} = \mathbf{E}_{\text{ext}} + \mathbf{E}_{\text{int}}$ , with the external field given by equation (4) as before. The magnetic field Our set of differential equations in equation (9) now get an additional term, and for a particle  $i$ , the equations become

$$\ddot{x}_i - \omega_{0,i}\dot{y}_i - \frac{1}{2}\omega_{z,i}^2 x_i - k_e \frac{q_i}{m_i} \sum_{j \neq i} q_j \frac{x_i - x_j}{|\mathbf{r}_i - \mathbf{r}_j|^3} = 0, \quad (21a)$$

$$\ddot{y}_i + \omega_{0,i}\dot{x}_i - \frac{1}{2}\omega_{z,i}^2 y_i - k_e \frac{q_i}{m_i} \sum_{j \neq i} q_j \frac{y_i - y_j}{|\mathbf{r}_i - \mathbf{r}_j|^3} = 0, \quad (21b)$$

$$\ddot{z}_i + \omega_{z,i}^2 z_i - k_e \frac{q_i}{m_i} \sum_{j \neq i} q_j \frac{z_i - z_j}{|\mathbf{r}_i - \mathbf{r}_j|^3} = 0. \quad (21c)$$

To simplify the analysis, we will neglect any other contribution affecting the motions of the particles inside the trap.

## III. METHODS

### A. Numerical implementation and integration

We aim to create a program in C++ that simulates a set of  $N_p$  particles inside a Penning trap. An object-oriented code is befitting this task and we present in the following descriptions of the classes `Particle` and `PenningTrap`.

The purpose of `Particle` is to hold the parameters, such as the position, of a particle. We let an object of this class be initialised with a charge  $q$ , a mass  $m$ , a

position  $\mathbf{r} = (x, y, z)$  and a velocity  $\mathbf{v} = (v_x, v_y, v_z)$ . We add functions to update the latter two.

The `PenningTrap`-class imitates the physical system that is the Penning trap of external electric and magnetic fields according to eqs. (6) and (7), and characteristic dimension  $d$ . It is friend with the `Particle`-class and, in order to resemble the physical situation as much as possible, accepts only input particles of this type. When filled with  $N_p \geq 1$ , an object of `PenningTrap` is ready to simulate the evolution of the `Particle` object(s) for a given period of time and time step size with either a forward Euler or a fourth order Runge-Kutta numerical scheme.

Some more here?

Rewrite the below list. Should not be bullet points. Should perhaps not introduce features that are not yet relevant for the report, e.g. time-dep potential is not mentioned yet.

`PenningTrap` includes several additional functionalities. Amongst other things, the class

- offers the choice between RK4 or FE integration method.
- provides the option to include or exclude Coloumb interactions in the simulation, as they are computationally greedy.
- includes a method for adding a time-dependent perturbation to the external electric potential,  $V_0 \rightarrow V_0(1 + f \cos(\omega_V t))$ .
- has the ability to count the number of particles still trapped, that is the number particles whose position  $\mathbf{r}$  is such that  $|\mathbf{r}| \leq d$ .
- can generate a set of identical particles with positions and velocities that are normally distributed within the trap's dimensions.

#### Numerical integration

The equation of motion (2) is split into two first order ODEs as follows:

$$\begin{aligned} \dot{\mathbf{v}} &= \frac{\mathbf{F}}{m} \\ s\dot{\mathbf{r}} &= \mathbf{v} \end{aligned} \quad (22)$$

We then get six discretised equations to solve for each particle at each step in time. We use two different approaches when solving equations 22 numerically. Both methods are single step methods, meaning we advance one time step per iteration. The simpler method, FE [1] is of first order meaning that we advance one time step by considering the gradient at the current time step only. This results in few FLOPs per iteration. Hence, this scheme offers numerical efficiency. The draw back

is the accuracy of the resultant solution. For a step size  $h$ , the FE scheme has a local truncation error of  $\mathcal{O}(h^2)$  which results in a global error  $\mathcal{O}(h)$ . Since we want  $h$  to be small, the global error is large compared to the local error.

The second, more advanced method is the RK4 methods [1], which is of fourth order. This means that we advance one time step by considering the gradient four times across a single time step. The gradient we use to advance the solution is a superposition of the four previously found gradients. This results in many FLOPs per iteration. Hence, this scheme is numerically more expensive than the FE scheme. However, it offers a far more accurate solution yielding a local truncation error of  $\mathcal{O}(h^5)$  and global error  $\mathcal{O}(h^4)$ . Again, since  $h$  is small, these errors are four magnitudes smaller than those of the FE scheme. Mention RK4 may be more efficient, since smaller  $h$  gives fewer iterations?

#### B. Penning trap parameters and particle properties

For the Penning trap parameters, we choose the following numerical values:

$$d = 500 \mu\text{m}$$

$$V_0 = 25.0 \text{ mV}$$

$$B_0 = 1.00 \text{ T}$$

We convert all quantities to the following set of base units:

$$\text{Unit-length} = \text{one micrometre} = 1 \mu\text{m}$$

$$\text{Unit-time} = \text{one microsecond} = 1 \mu\text{s}$$

$$\text{Unit-mass} = \text{one atomic mass unit} = 1 \text{ u}$$

$$\text{Unit-charge} = \text{one elementary charge} = 1 \text{ e}$$

The particles we consider are Calcium ions ( $\text{Ca}^+$ ) with charge  $q = 1 \text{ e}$  and mass  $m = 40.078 \text{ u}$ . These values ensure that the condition in equation (15) is fulfilled.

#### C. Initial conditions

For simulations of one or two particles, we use the following initial conditions:

- Particle 1

$$\mathbf{r}_0^{(1)} = (20, 0, 20) \mu\text{m}$$

$$\mathbf{v}_0^{(1)} = (0, 25, 0) \mu\text{m}/\mu\text{s}$$

- Particle 2

$$\mathbf{r}_0^{(2)} = (25, 25, 0) \mu\text{m}$$

$$\mathbf{v}_0^{(2)} = (0, 40, 5) \mu\text{m}/\mu\text{s}$$

### D. Single particle simulation

We begin by simulating a single particle, using the initial conditions for Particle 1 in section III C. We compare the resulting axial motion obtained from FE and RK4 with the analytical solution in equation (10) which has the specific solution

$$z(t) = z_0 \cos(\omega_z t), \quad (23)$$

where  $z_0 = 20 \mu\text{m}$ . We simulate over a duration of  $T_1 = 50 \mu\text{s}$ , using  $n_1 = 4000$  steps.

To study the accuracy of the two algorithms, we compute the size of the relative error of the two algorithms as a function of time for a duration of  $T_1$ . To study the step size dependency, we do this for four different time steps:

$$n_1 = 4000$$

$$n_2 = 8000$$

$$n_3 = 16000$$

$$n_4 = 32000$$

The size of the error is given by

$$\Delta_{\text{rel},k} = \frac{|\mathbf{r}_{\text{exact}} - \mathbf{r}_k|}{|\mathbf{r}_{\text{exact}}|} \quad (24)$$

where  $\mathbf{r}_{\text{exact}}$  is the analytical solution. For the movement in the  $xy$ -plane, the specific solution for  $f(t)$  is given by equation (13) with

$$A_+ = \frac{v_0 + \omega_- x_0}{\omega_- - \omega_+}, \quad A_- = -\frac{v_0 + \omega_+ x_0}{\omega_- - \omega_+}, \quad (25)$$

$$\phi_+ = 0, \quad \phi_- = 0,$$

where  $v_0 = \dot{y}(0) = 25 \mu\text{m}/\mu\text{s}$  and  $x_0 = 20 \mu\text{m}$ .  $z(t)$  is given by equation (23).

Using the results of the estimated errors, we will estimate the error convergence rate,  $r_{\text{err}}$  for our two algorithms

$$r_{\text{err}} = \frac{1}{3} \sum_{k=2}^4 \frac{\log(\Delta_{\text{max},k}/\Delta_{\text{max},k-1})}{\log(h_k/h_{k-1})}, \quad (26)$$

where  $h_k = T_1/n_k$  is the step size and

$$\Delta_{\text{max},k} = \max_i |\mathbf{r}_{i,\text{exact}} - \mathbf{r}_i| \quad (27)$$

is the maximum size of the absolute error with  $n_k$  time steps.

#### 1. Two particles

Having studied the accuracy of our solver, we proceed by studying two particles in the Penning trap with the

initial conditions specified in section III C. For  $n_2 = 8000$  timesteps we simulate the two particles over a duration of  $T_1$ , both with and without interactions, using the RK4 method. In both cases, we will study the motion of the two particles in the  $(x, y)$ -plane, their trajectories in the  $(x, v_x)$ -plane and the  $(z, v_z)$ -plane and a 3D plot showing their trajectories in  $(x, y, z)$  space.

### E. Many particles - Resonance

Now that the basics of our Penning trap is complete, we explore resonance features of our trap when we have a large number of particles in the trap. To do this, we subject the system to a time-dependent electromagnetic field by making the replacement

$$V_0 \rightarrow V_0(1 + f \cos(\omega_V t)), \quad (28)$$

where  $f$  is a constant amplitude and  $\omega_V$  is the angular frequency of the time-dependent potential. Using this potential, we will consider  $N_p = 100$  particles with normal distributed initial positions and velocities with a mean of zero and variance  $\sigma^2 = 1$ . The magnitude of each particle's initial position and velocity vector is  $d/10$ . To find potential resonance frequencies, we will plot the fraction of particles that are left in the trap after a duration of  $T_2 = 500 \mu\text{s}$ <sup>1</sup> as a function of applied frequency  $\omega_V \in (0.2, 2.5)$  MHz. For this broad frequency range we use a step size of 0.02 MHz for the applied frequencies and switch off the interactions between the particles. We plot the result for the three amplitudes  $f = 0.1, 0.4, 0.7$ , using  $n = 80000$  time steps. Using only the RK4 scheme, we perform two sorts of frequency scans:

- (i) **Broad-band resonance search:** Run many simulations with interactions switched *off* for a broad range of frequencies, but with equal magnitude of the perturbation. Log the number of particles remaining in the trap after each simulation.
- (ii) **Narrow-band resonance search:** Run several simulations with interactions turned *on* for a narrow range of frequencies. The band is determined using the result of (i) to locate a small range of response frequencies. Repeat with interactions turned *off* for comparison. Make sure the grid of frequencies is fine-grained compared to the one in (i). **Rephrase** Repeat for interactions turned *off* for comparison. Write down the number of particles trapped at  $T_2$ .

Having completed a broad frequency search, we proceed by

---

<sup>1</sup> Strictly speaking, some of them are stopped before this due to an empty trap, but the result is the same.



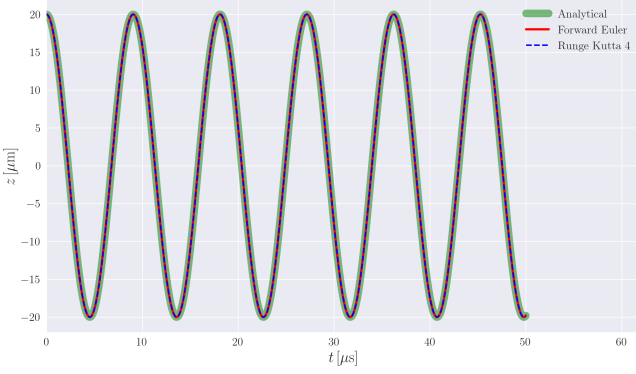


FIG. 2. Movement in the  $z$ -plane for a single particle, simulation for  $50 \mu\text{s}$  with  $n_1 = 4000$  time steps. The analytical solution from equation (10) is plotted in green, and the integrated solutions using the forward Euler and Runge-Kutta 4 scheme is shown in red and blue respectively. Initial conditions are those of Particle 1, given in III C.

## IV. RESULTS

### A. Single particle

We start by simulating a single particle, Particle 1, with initial conditions given in III C. The duration of the simulation is set to  $T_1$  and we use  $n_1$  time steps. In Figure 2 we plot the  $z$ -component of the position as function of time. The solutions are found both using the FE and RK4 schemes, shown in red and blue respectively. FE and RK4 defined shortening earlier? - Yes, in introduction:). The analytical solution, found from equation (10) where the initial conditions yield  $c_1 = z_0 = 20 \mu\text{m}$  and  $c_2 = v_{z,0}/\omega_z = 0$  is shown with green in the figure.

Since both FE and RK4 are approximations of the analytical solution we expect them to have a relative error compared with it. We repeat the simulations using  $n_2, n_3$  and  $n_4$  time steps and find the relative error at each time step according to (reference to relative error formula). The results are shown in Figures 3 and 4. We note that for an increasing time step, the relative time step decrease, and the error for the RK4 scheme is significantly less than that of FE. (ref some previous discussion with hs?)

We compute the convergence rate at according to equation (26) and find that  $r_{\text{err}} \simeq 3.9$  for RK4 and that  $r_{\text{err}} \simeq 1.4$  for FE. What is dis

### B. Two particles

We simulate Particle 1 and Particle 2 for duration  $T_1$ , using  $n_2$  time steps. This is a trade off between numerical accuracy and computation time, since we now use the RK4 method (Or do we use both?), both with and without Coulomb interactions. For the three figures soon to be mentioned, Particle 1 is shown in blue, Particle 2 in

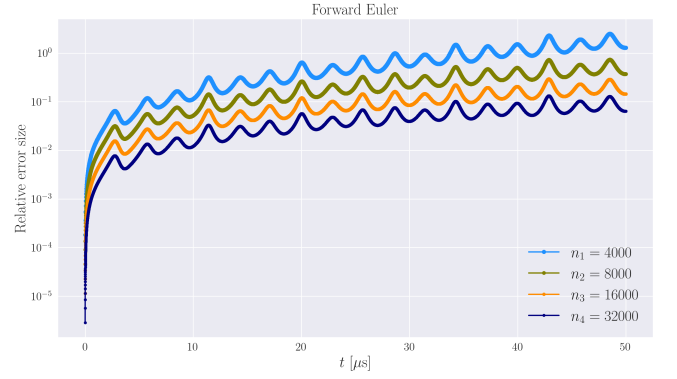


FIG. 3. Relative error of the forward Euler scheme, simulated for  $50 \mu\text{s}$ , for a different amount of steps  $n_k$  as indicated in the figure legend. Pay attention to the logarithmic  $y$ -axis.

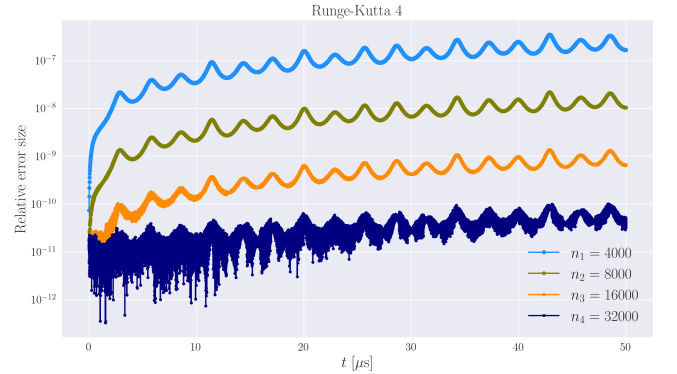


FIG. 4. Relative error of the Runge-Kutta 4 scheme, simulated for  $50 \mu\text{s}$ , for a different amount of steps  $n_k$  as indicated in the figure legend. Pay attention to the logarithmic  $y$ -axis.

red, initial conditions are as specified in section III C and the start and end point of their trajectories are indicated with a cross and a star respectively. Figure 5 show the movement of the two particles in the  $xy$ -plane. The left panel when we have no Coulomb interaction, and the right panel when they interact.

Figure 6 show the phase plots of the two particles along the  $x$ -axis, and Figure 7 along the  $z$ -axis.

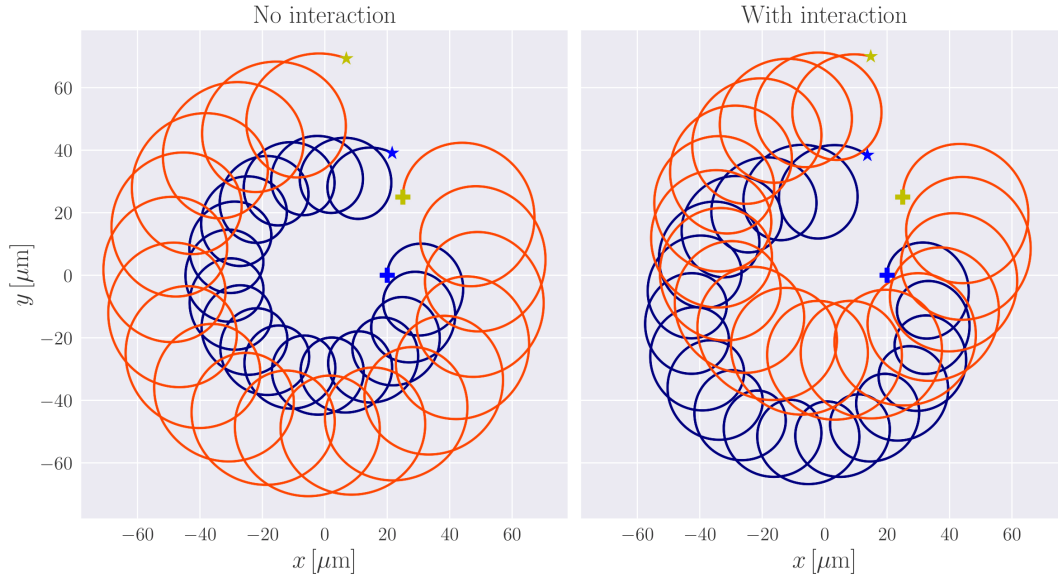


FIG. 5. Movement of two particles in the  $xy$ -plane simulated for  $50 \mu\text{s}$ . The left panel show their trajectories computed without particle interaction. In the right panel we have allowed for the particles to interact. We have used the Runge-Kutta 4 scheme to obtain these trajectories. Particle 1 is shown in blue, and Particle 2 in green. Both panels use the same initial conditions as specified in section III C. The starting points of their trajectories are indicated with a cross, their ending points with a star.

### C. Many particles

Three broad-band scans are performed, one for each of the amplitudes  $f = 0.1, 0.4$ , and  $0.7$ . In particular, we run 300 simulations where we use the same amplitude  $f$  and for each run, apply a different frequency  $\omega_V \in [0.2, 2.5]$  MHz. We reused the time step size from section IV B. The fraction of particles remaining is presented in Figure 9 as a function of applied frequency.

For the next step, we choose the smallest amplitude and the middlemost response in Figure 9, i.e.  $f = 0.1$  and  $\omega_V \in [1.35, 1.45]$  MHz. We run 50 simulations, each with slightly different applied frequency, for which interactions forces are included. The number of steps is reduced to 20000 in this case, corresponding to a step size  $2T_1/n_1$  (twice that of the first simulation in section IV A). We repeat for negligible interactions. Figure 10 shows  $N_{\text{trapped}}$  as a function of  $\omega_V$  in both cases.

## V. DISCUSSION

We provide the movement in the  $z$ -direction in figure 2 as some sort of test to see whether the numerical integrations methods works or not. Hence, we use the fewest number of time steps,  $n_1$  in order reveal the largest potential errors. From the figure they seem to overlap perfectly, however there is reason to think the error in the calculated solutions grow with time. This is indeed the case, as the error for the small duration  $T_1$  is not visi-

ble due to the thickness of plotted lines and the scale of the plot. Although not shown here, if we were to zoom in on the graphs at a late time they do not overlap, i.e. indicating that there is an error although hard to spot. Nevertheless, the calculated solution seems to fit the analytical quite well, but we are still interested in quantifying the error, which we expect to be smaller if we increase the number of time steps.

Using the analytical solution as reference, the relative error as found from equation 24 is shown in figure 3 for the FE scheme and in figure 4 for the RK4 scheme. Here, all four time steps  $n_k, k \in [1, 4]$  is included. The increase in error for both plots as we increase the number of time steps seem to follow the order of the global error for each scheme. This also becomes apparent when considering the actual relative error in the plots ( $y$ -axis values), and the magnitudinal decrease in error when we increase the number of time steps. The latter is significantly more apparent for the RK4 scheme, which is to be expected as the global error should go as  $\mathcal{O}(h^4)$ , rather than  $\mathcal{O}(h)$  for the FE scheme. There is a noticeable increase in the widths of the different graphs for the RK4 scheme in figure 4. This can be explained by the small numerical values of the relative error, and the fact that we use a logarithmic  $y$ -axis which emphasize the variation for small errors (broad fuzzy looking graph for  $n_4$ ).

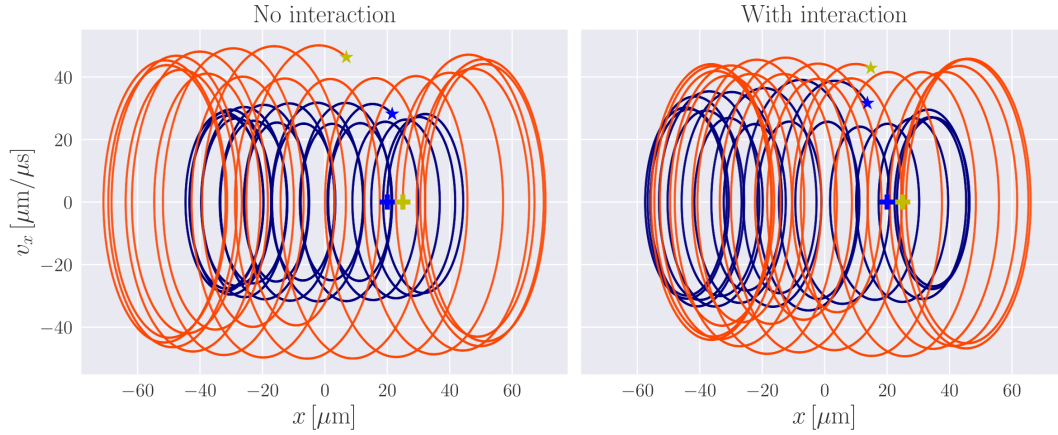


FIG. 6. Phase plots along the  $x$ -axis for two different particles simulated for 50  $\mu\text{s}$ . The left panel show their behaviour without interactions and the right panel with. Particle 1 is shown in blue, and Particle 2 in green. Both panels use the same initial conditions as specified in section III C. The starting points of their trajectories are indicated with a cross, their ending points with a star.

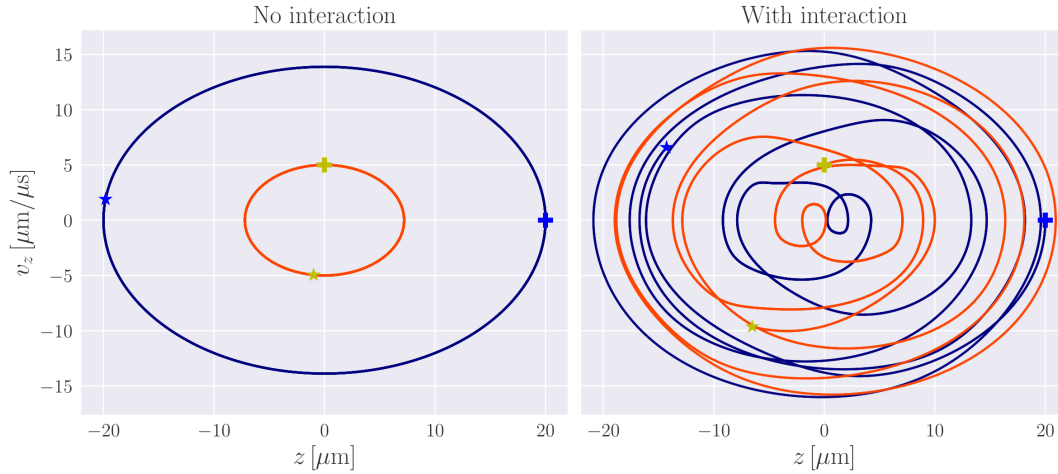


FIG. 7. Phase plots along the  $z$ -axis for two different particles simulated for 50  $\mu\text{s}$ . The left panel show their behaviour without interactions and the right panel with. Particle 1 is shown in blue, and Particle 2 in green. Both panels use the same initial conditions as specified in section III C. The starting points of their trajectories are indicated with a cross, their ending points with a star.

#### A. Adding a time-dependent perturbation to the potential

- Why these frequencies?

- Effect of increasing amplitude
- Effect of Coulomb interactions
- Comment on number of time steps

From Figure 9 we see how an oscillating electric potential gives rise to the escapement of particles in the



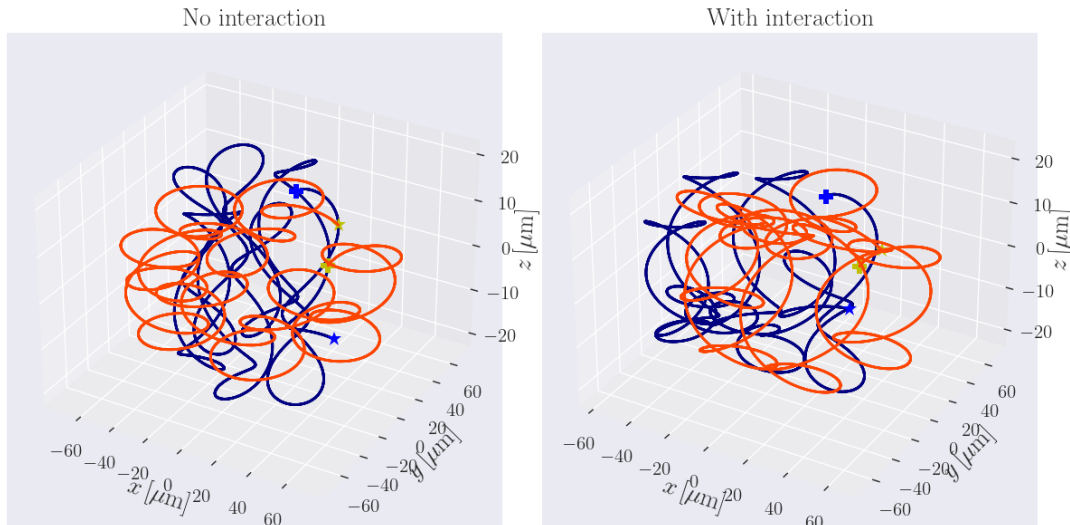


FIG. 8. The trajectory of Particle 1 (blue) and Particle 2 (orange) in the Penning trap for 50  $\mu\text{s}$ . The left panel shows the situation when we neglect interaction forces, whilst the right panel introduces these forces. The starting points of their trajectories are indicated with a cross, their ending points with a star.

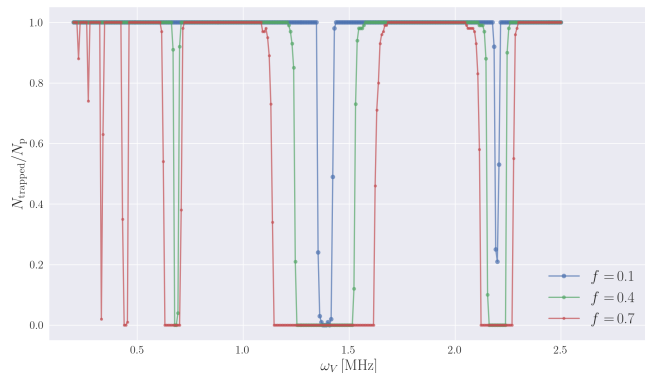


FIG. 9. Fraction of particles that are still trapped by the Penning trap after 500  $\mu\text{s}$ , as function of the applied frequency  $\omega_V$ , for different amplitudes  $f \in \{0.1, 0.4, 0.7\}$ , without considering particle interactions. All graphs are resulting from simulations using 80000 time steps.

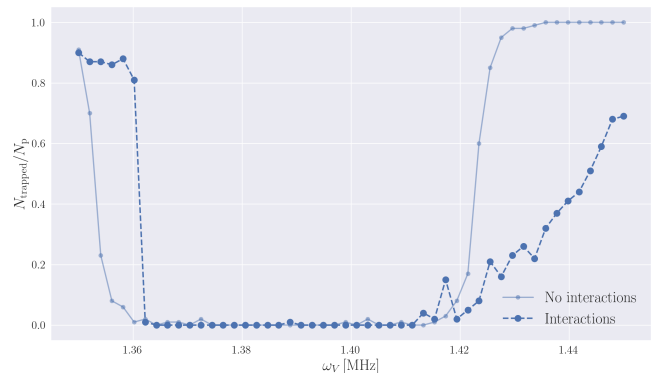


FIG. 10. Fraction of particles that are still trapped by the Penning trap after 500  $\mu\text{s}$ , as function of selected applied resonance frequencies  $\omega_V$ , with amplitude  $f = 0.1$ , both with and without particle interactions. Both graphs are resulting from simulations using 20000 time steps.

Penning trap. For some bands of applied frequencies, basically all particles have escaped before the simulation has ended. Increasing the magnitude of the perturbation has the effect of broadening these band widths, as well as to make them occur more frequently. The largest bands for which the simulations become unstable are ???

Without interactions, it seems to be the case that either all particles escape or stay trapped, referring to the steep graphs in Figures 9 and 10, but especially the latter as we see how it differs from the graph representing simulations with interacting particles. Interacting particles in a sense push the resonance frequencies upwards: they

demand higher frequencies in order for all to escape, but as the non-interacting particles are trapped again, the interacting particles are only partly trapped.

## VI. CONCLUSION

*In this section we state three things in a concise manner: what we have done, what we have found, and what should or could be done in the future.*



FIG. 11. Nanna, Johan and Vetle working on the project, respectively (from left to right), 2022 (colorized).

- 
- [1] Atkinson, K. E. (1989). *An Introduction to Numerical Analysis (Second Edition)*, chapter Six, pages 333–443. John Wiley & Sons.
  - [2] Dehmelt, H. G. (1989). Hans G. Dehmelt - Biographical. Retrived from: <https://www.nobelprize.org/prizes/physics/1989/dehmelt/biographical/> (Oct. 2022).
  - [3] Griffiths, D. J. (2017). *introduction to Electrodynamics (Fourth Edition)*, chapter 3 Potentials, page 118. Cambridge University Press.